BBA - Molecular Basis of Disease 1865 (2019) 2606–2617

Contents lists available at ScienceDirect

BBA - Molecular Basis of Disease

journal homepage: www.elsevier.com/locate/bbadis

Peli1 induction impairs cardiac microvascular endothelium through Hsp90 dissociation from IRE1α

Qianwen Zhao[a], Jie Yang[a], Hao Chen[a], Jiantao Li[a], Linli Que[a], Guoqing Zhu[a], Li Liu[b], Tuanzhu Ha[c], Qi Chen[a], Chuanfu Li[c], Yong Xu[a,*], Yuehua Li[a,*]

[a] Key Laboratory of Targeted Intervention of Cardiovascular Disease, Collaborative Innovation Center for Cardiovascular Disease Translational Medicine, Nanjing Medical University, Nanjing 211166, Jiangsu, China
[b] Department of Geriatrics, The First Affiliated Hospital of Nanjing Medical University, Nanjing 210029, China
[c] Department of Surgery, East Tennessee State University, Campus Box 70575, Johnson City, TN 37614-0575, USA

ARTICLE INFO

Keywords:
Cardiac microvascular endothelial injury
Hsp90
IRE1α
Peli1

ABSTRACT

Ameliorating cardiac microvascular injury is the most effective means to mitigate diabetes-induced cardiovascular complications. Inositol-requiring 1α (IRE1α), a sensor of endoplasmic reticulum stress, is activated by Toll like receptors (TLRs), and then promotes cardiac microvascular injury. Peli1 is a master regulator of TLRs and activates IRE1α. This study aims to investigate whether Peli1 in endothelial cells promotes diabetes-induced cardiac microvascular injury through activating IRE1α. Here we found that Peli1 was markedly up-regulated in cardiac endothelial cells of both diabetic mice and in AGEs-treated cardiac microvascular endothelial cells (CMECs). Peli1 deficiency in endothelial cells significantly alleviated diabetes-induced cardiac microvascular permeability, promoted microvascular regeneration, and suppressed apoptosis, accompanied by the attenuation of adverse cardiac remodeling. Furthermore, Peli1 deletion in CMECs ameliorated AGEs-induced damages in vitro. We identified heat shock protein 90 (Hsp90) as a potential binding partner for Peli1, and the Ring domain of Peli1 directly bound with Hsp90 to enhance IRE1α phosphorylation. Our study suggests that blocking Peli1 in endothelial cells may protect against diabetes-induced cardiac microvascular injury by restraining ER stress.

1. Introduction

Cardiac vascular complications are considered to be the major cause of high morbidity and mortality in diabetic patients [1,2]. In the progression of diabetes, cardiac microvascular impairment occurs before macrovascular injury and renders the heart more susceptible to ischemic damages [3,4]. Accumulating evidence indicates that hyperglycemia impairs endothelial integrity, leading to severe damages on small arteries and capillaries with the involvement of oxidative stress and inflammatory response [5]. In addition, microvascular injury impairs the formation of new small arterioles and capillaries, contributing to cardiac hypertrophy due to the altered metabolism [6]. Therefore, it is generally accepted that hyperglycemia-induced microvascular injury is an important cause of diabetic cardiomyopathy.

Multiple pathological factors, such as oxidative stress and inflammatory responses [7,8], are involved in cardiac microvascular injury in diabetes and serve as cellular stresses to induce the unfolded protein response (UPR) [9,10]. Although UPR is an adaptive response to cellular stresses, the excessive UPR, namely endoplasmic reticulum (ER) stress, triggers a stress cascade with pathological consequences including oxidative stress and apoptotic responses in specialized cells and tissues. ER stress is activated in microvascular injury under diabetic conditions [11,12], and the sensor protein inositol-requiring enzyme 1 alpha (IRE1α) plays a crucial role in diabetic microvascular injury [13–15]. ER stress is induced by IRE1α activation to impair the permeability of blood-brain barrier through JNK-mediated apoptosis. In

Abbreviations: AGEs, advanced glycation end products; ATF-4, activating transcription factor-4; ATF-6, activating transcription factor-6; CMECs, cardiac microvascular endothelial cells; CHOP, CAAT/enhancer-binding protein homologous protein; EF, ejection fraction; ER, endoplasmic reticulum; FS, fractional shortening; GRP78, glucose regulated protein 78; Hsp90, heat shock protein 90; IL-1R, Interleukin-1 receptor; IRE1α, inositol-requiring 1α; MACS, Magnetic-activated cell sorting; MDS, molecular dynamics simulation; MI, myocardial infarction; PERK, protein kinase RNA-like ER kinase; STZ, streptozotocin; TEER, Transendothelial electrical resistance; TLRs, Toll-like receptors; TNFR1, TNF-α receptor 1; TRAF6, TNF receptor associated factor 6; UPR, unfolded protein response; VE-cad, vascular endothelial-cadherin; VEGF, Vascular endothelial growth factor; XBP1, X-box binding protein 1

* Corresponding authors at: Key Laboratory of Targeted Intervention of Cardiovascular Disease, Nanjing Medical University, Nanjing 211166, China.
E-mail addresses: yjxu@njmu.edu.cn (Y. Xu), yhli@njmu.edu.cn (Y. Li).

https://doi.org/10.1016/j.bbadis.2019.06.017
Received 28 February 2019; Received in revised form 10 June 2019; Accepted 25 June 2019
Available online 29 June 2019

addition, IRE1α activation accelerates the degradation of intracellular VEGF through promoting XBP1 mRNA splicing to damage vascular regeneration. The stability of IRE1α is determined by the association with cytosolic chaperone protein heat shock protein 90 (Hsp90), and IRE1α could be activated when detached from Hsp90 by oligomerization [16]. This finding establishes a signal transduction cascade for Hsp90 to regulate ER stress, potentially involved in endothelial dysfunction.

In diabetes, hyperglycemia promotes the glycation of protein and impairs endothelial homeostasis. Advanced glycation end products (AGEs) are glycated proteins or lipids with long term-exposure to hyperglycemia that are prevalent in the diabetic vasculature, contributing cardiovascular complications [17]. AGEs accumulation leads to the activation of Toll-like receptors (TLRs), interleukin-1 receptor (IL-1R) and TNF-α receptor 1 (TNFR1), mediating inflammation and apoptotic responses [18–20]. It has been demonstrated that inhibiting TNFR1 in human lung microvascular endothelium is able to retard endothelial apoptosis to protect microvascular function [21]. Moreover, IRE1α is phosphorylated by TLR2/4 and TNFR1 to induce ER stress, resulting in endothelial dysfunction [22,23]. Since apoptosis is a downstream consequence of ER stress, these events suggest that AGEs induce apoptosis and impair endothelial integrity and function by activation of ER stress.

Pellino proteins are evolutionary conserved scaffold proteins in TLRs/IL-1R and TNFR1 signalings and three isoforms are identified in mammalian cells, termed Peli1, 2, 3 [24]. Peli1 promotes the nuclear translocation of p65 and mediates inflammatory responses by interacting with IL-1R-accociated kinase1 (IRAK1) [25]. Moreover, Peli1 could bind to TNF receptor associated factor 6 (TRAF6) [26]. Because TRAF6 is implicated in UPR to promote the ubiquitination and subsequent phosphorylation of IRE1α [27], this event raises the possibility that Peli1 mediates ER stress and subsequent consequences through regulating of the stability of IRE1α. Therefore, we hypothesize that Peli1 in endothelial cells aggravates cardiac microvascular injury in diabetic mice. Thus, in this study, we explore whether Peli1 deficiency in endothelial cells afforded protection against diabetic-induced cardiac microvascular injury via suppression of ER stress in diabetic mice and the underlying molecular mechanisms were detected.

2. Materials and methods

2.1. Animals

Male C57BL/6 mice aged 8–10 weeks were purchased from the Model Animal Research Center of Nanjing University (Nanjing, China). Peli1$^{Flox/Flox}$ (Peli1$^{F/F}$) mice were developed previously [28,29]. Peli1$^{F/F}$ mice were crossed to Tie2-Cre mice to generate Tie2-cre Peli1$^{Flox/+}$ mice. Then, the endothelium Tie2-Cre Peli1$^{Flox/Flox}$ (Peli1$^{\Delta EC}$) mice were generated by brother–sister mating. Similarly, systemic knockout mice (Peli1^{KO}) were developed with Peli1$^{F/F}$ mice and Ddx-4-Cre mice. All animal experiments were carried out in accordance with the Guide for the Care and Use of Laboratory Animals prepared by the National Academy of Sciences and published by the National Institutes of Health (NIH Publication No. 85-23, revised in 1996) and was approved by the Nanjing Medical University Committee on Animal Care (Permit Number: IACUC 14030103).

2.2. Induction of diabetic model

Diabetes was induced by intraperitoneal injection of streptozotocin (STZ, 50 mg/kg in 10 mmol/L citrate buffer at pH 4.6) for 5 consecutive days. Control mice received the same volume of citrate buffer (0.1 M Na citrate, PH 4.5). Blood glucose levels were detected 1 week after injection and values ≥16.6 mmol/L were considered as diabetes. Then the blood glucose (Johnson & Johnson, New Brunswick, USA) and body weight were detected once per month. The levels of AGEs in serum were measured according to the corresponding AGEs assay kit (catalog: #K929-100, Biovision, Milpitas, CA, USA).

2.3. Cell isolation, culture and identification

Cardiac microvascular endothelial cells (CMECs) were isolated as previously described [30]. Male C57BL/6J (20–25 g) mice, Peli1$^{F/F}$ mice (20–25 g) and Peli1^{KO} (20–25 g) were rapidly excised after anesthetized with ether. Cells were then re-suspended in endothelial basal medium-2 containing 10% FBS premixed with endothelial cell growth supplements following the manufacturer's instructions. For further details, see Electronic supplementary materials (ESM) Methods.

2.4. Echocardiography to assess cardiac function

Echocardiography was performed as described in our previous study [31] with a two-D guide M-mode transthoracic echocardiographic examination (General Electric Co., Fairfield, CT, USA). Mice were anesthetized with isoflurane (1.5% with O_2 1L/min). Cardiac function was measured 16 weeks after diabetes. All measurements were detected by a single echocardiographer who was blinded to the whole experiments.

2.5. Permeability of CMECs

The permeability in CMECs was determined by Transendothelial electrical resistance (TEER) measurement. Cells were diluted into PBS, which were supplemented with 0.1% fatty-acid free BSA and flux measurements described by using 4-kDa FITC-dextran (1 mg/mL) [32]. For further details, see ESM Methods

2.6. TUNEL assay

Apoptosis level was detected by the terminal deoxynucleotidyl transferase (TdT)-mediated dUTP nick end-labeling (TUNEL) assay and fluorescence microscopy was used to observe the TUNEL-positive apoptosis cells (see ESM for detailed Methods).

2.7. Immunofluorescence staining

CMECs were seeded in glass bottom dish (35 mm dish with 14 mm bottom well). Then the cells were fixed with 4% paraformaldehyde for 4 h at 4 °C before permeabilized with 0.1% Triton X-100 for 10 min. After washed with PBS for three times, CMECs were blocked with 5% BSA for 20 min at room temperature. Immunostaining was performed with the indicated primary antibodies (anti-p-IRE1α). The cells were washed with PBS and the nuclei were stained with DAPI after incubating with appropriate secondary antibodies.

2.8. Immunoprecipitation and western blot analysis

Immunoprecipitation and western blot analysis were performed by using p-IRE1α, IRE1α, Peli1, p-PERK, PERK, ATF6, hsp90, p-p38, p38, p-JNK. JNK, AGEs, caspase12, caspase3, TRAF2, HA, Flag and Tubulin antibodies (see ESM Methods).

2.9. Integrity of cardiac microvessels

Microvascular endothelial integrity of mice's hearts was examined with scanning electron microscopy. Prepared samples were subsequently observed by a scanning electron microscope (Hitachi S-3400N). For further details, see ESM Methods.

2.10. Permeability of cardiac microvessels

Cell-to-cell junctions were assessed with Transmission electron microscopy as previously described [33]. Hearts of anesthetized mice

were perfused via the aorta with prefixative solution and then the hearts were perfused with fixing solution using a Langendorff system. Subsequently, tissue samples were dehydrated by graded ethanol and embedded in Agar 100. For further details, see ESM Methods.

2.11. Tube formation assay

The formation of capillary-like structures was assessed in a 24-well plate using a growth factor-reduced Matrigel (BD Biosciences), which then visualized and captured by using a phase-contrast inverted microscope equipped. For further details, see ESM Methods.

2.12. RNA quantification

The relative expression levels of mRNA of mice *Peli1*, *Ve-cadherin*, *Pecam-1* and *Gapdh* were quantified by quantitative RT-PCR (see ESM Methods).The data were analyzed by using the $2^{-\Delta\Delta C}$ method and normalised to endogenous control Gapdh mRNA.

2.13. Construct glutathione S-transferase (GST) fusion proteins and GST pull-down assay

GST fusion proteins of GST-Peli1, GST-Peli1ΔRing and GST-Peli1ΔFHA were expressed in Trans1-T1 Phage Resistant Chemically Competent Cells (TransGen, Beijing, China), which were induced with 0.1 mM isopropyl-1-thio-β-D-galactopyranoside (Amresco, Solon, Ohio, USA) for 16 h at 28 °C. To get further study in the binding domain of Peli1 to Hsp90 in vitro, purified GST-Peli1, GST-Peli1ΔRing and GST-Peli1ΔFHA proteins were incubated with equal molar amounts of HA-Hsp90 by rocking at 4 °C for 3 h before incubating with Glutathione Agarose beads (Thermo Scientific, Rockford, USA) for 1 h at 4 °C. Then, the binding proteins eluted in SDS loading buffer were extracted and analyzed by western blot.

2.14. Silver staining and mass spectrometry

The Flag protein complexes in the cell lysates were captured by using anti-Flag Beads. Then the magnetic beads were washed and Flag peptide was applied to elute the Flag-protein complex. Bands were excised from the gel and subjected to in-gel tryptic digestion. Resulting peptides were separated by reverse-phase liquid chromatography on an easy-nLC 1000 system and directly sprayed into a QExactive mass spectrometer. For further details, see ESM Methods.

2.15. Magnetic-activated cell sorting (MACS)

Hearts from Peli1$^{F/F}$ and Peli1$^{\Delta EC}$ mice under diabetic and non-diabetic condition were rinsed and digested with 0.2% collagenase II and 0.2% trypsin using gentle MACS dissociator, following the manufacturer's instruction. Endothelial cells were immunomagnetic sorted using CD31 antibody (Miltenyi Biotech), as reported in previous research [34]. Purity of cell preparations was detected by flow cytometry using CD31-PE antibody (Miltenyi Biotech).

2.16. Scratch-wound assay

In each well of 6-well plate, a straight scratch was made by a pipette tip to form a 'wound' through the middle of 100% confluent CMECs monolayer. CMECs were transfected with or without adv-shPeli1 or adv-Scr and then the cells were treated with 0.1% FBS EBM-2 basal medium with or without AGEs. After 8 h incubation, the migration of CMECs into the 'wound' area was quantified as mean number of the migrated cells.

2.17. Structure modeling and Peli1-Hsp90 binding prediction

ZDOCK was used to imitate protein-protein docking. Prepare protein mocule and remove irrelevant ligands, water molecules and ions before adding all hydrogen atoms and CHARMm force fields. According to the docking protocol, the Peli1 protein was docked onto the protein Hsp90 using ZDOCK software. The scores of the first 2000 structures are output and the clustering analysis of these 2000 structures is performed based on the clustering conditions with the RMSD cutoff value of 10.0 Å. In all docking, searching possible docking conformations and selecting the most representative of the first 10 categories, the optimal score of the Peli1 conformation identified as the selected conformation.

2.18. Molecular dynamics simulation (MDS) and protein-ligand interaction analysis during MD simulation

The complex of Hsp90 protein and Peli1 protein was assembled using the aforementioned molecular docking model. In the simulation system construction, the FF99SB force field of AMBER was used, as well as adding a TIP3P water model of 10.0 Å from the edge of the composite, the periodic boundary and counterions. For further details, see ESM Methods.

2.19. Statistical analysis

The samples were randomized and special method of randomization for all experiments. Experiments were also blind to group assignment and outcome assessment for all experiments. No data, samples or animals were excluded from the reported results. Data are shown as means ± SEM. Statistical comparisons were used *t*-test, one-way or two-way ANOVA with Bonferroni multiple comparison post-test. The data were analyzed with the GraphPad Prism-6 statistical software (Prism v6.0; GraphPad Software, La Jolla, CA, USA).Values of $p < 0.05$ were considered statistically significant in all experiments.

3. Results

3.1. Peli1 was up-regulated in both cardiac endothelial cells of diabetic mice and AGEs-treated CMECs

Mice were given intraperitoneal injection of STZ to induce diabetes, evidenced by persistent hyperglycemia with loss of body weight (Fig. 1a,b), as early as 10 day after last injection. At 8 week, significant amounts of AGEs were detectable in the serum, an indicator of protein glycation due to the long-term exposure to hyperglycemia (Fig. 1c). Compared with control, the protein and mRNA levels of Pelil were significantly higher in STZ-challenged mice's endothelial cells isolated from hearts at 8 week (Fig. 1d,e). To confirm the direct impact of AGEs on the expression of peli1, we detected the protein and mRNA levels of Peli1 in AGEs-treated CMECs. The CMECs isolated from the wild type mice displayed cobblestone-like morphology with positive staining of Dil-acetylated low-density lipoprotein intake and labeled CD31, ensuring the purity of CMECs (Fig. 1f). Peli1 protein and mRNA levels in CMECs were shown to increase in a time-dependent manner with AGEs stimulation (Fig. 1g,h). These results indicated that hyperglycemia or AGEs promoted Peli1 induction in the endothelium of myocardial microvessels.

3.2. Endothelial specific deficiency of Peli1 attenuated cardiac microvascular injury

To determine the possible impact of endothelial Peli1 in microvascular injury under diabetic conditions, we crossbred the Peli1-flox strain with the Tie2-Cre strain for specifical deletion of Peli1 in vascular endothelial cells (Peli1$^{\Delta EC}$). Firstly, First, primary cardiac microvascular endothelial cells (CD31^{+}) and non-EC cells (CD31^{-}) from

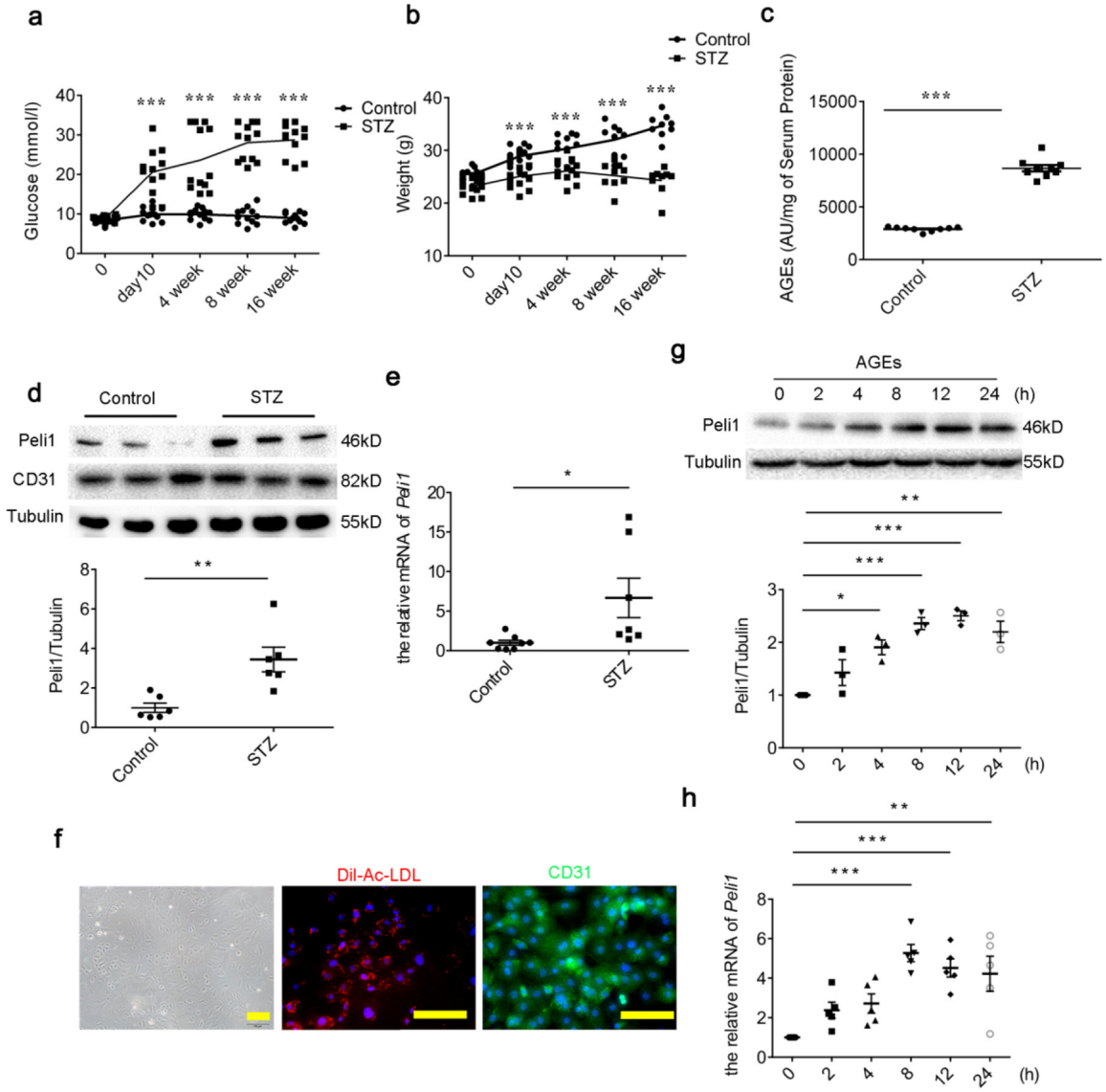

Fig. 1. Peli1 is upregulated in the myocardial microvascular endothelial cells under diabetic conditions. Diabetes was induced by the injection of streptozotocin (STZ) in C57BL/6 mice, and endothelial cells of myocardial were separated through Magnetic-activated cell sorting (MACS). WT mice were induced to diabetes for 10 day, 4 week, 8 week and 16 week after final injection. (a) Levels of fasting blood glucose; n = 12. (b) Body weight; n = 12. (c) Serum levels of advanced glycation end products (AGEs) in diabetic mice at 8 week. n = 9. (d) The protein expression of Peli1, CD31 and Tubulin were analyzed by western blots using Tubulin as a loading control at 8 week. n = 6. (e) RNA isolated from endothelial cells of myocardial was used to measure Peli1 expression by real-time quantitative PCR at 8 week. n = 6. (f) Representative images cardiac microvascular endothelial cells (CMECs) by phase-contrast microscopy (Scale bar, 40 μm, left). Uptake of Dil-acetylated low-density lipoprotein (Dil-Ac-LDL) by immunofluorescence (red, Dil-Ac-LDL, Scale bar, 50 μm, middle); Representative microscopy images of immunofluorescence staining for CD31 and DAPI. (Green, CD31, Scale bar, 50 μm, right). The protein (g) and mRNA (h) levels of *Peli1* in CMECs stimulated with AGEs (200 μg/mL) for different times were detected by western blot analysis and real-time quantitative PCR. n = 3–5. Data are expressed as mean ± SEM. $^{*}p < 0.05$, $^{**}p < 0.01$ and $^{***}p < 0.001$.

Peli1$^{\Delta EC}$ mice and Peli1$^{F/F}$ mice were isolated through MACS. Peli1 expression in CD31^{+} cells was diminished in Peli1$^{\Delta EC}$ mice compared with Peli1$^{F/F}$ mice, while the expression of Peli1 in CD31^{-} cells did not differ between the two groups with high level (Fig. 2a). As shown in Fig. 2b, under diabetic conditions, the integrity of microvessels was impaired in Peli1$^{F/F}$ mice, indicated by the morphological abnormalities; however, the morphological appearance of microvessels in Peli1$^{\Delta EC}$ mice remained virtually unchanged, indicating that endothelial specific deficiency of Peli1 protected the microvascular integrity. The microvascular barrier function was measured by Lanthanum nitrate perfusion and the impaired function was observed as evidenced by paracellular diffusion from the endothelium to the barrier in diabetic mice. The microvascular barrier dysfunction was attenuated in Peli1$^{\Delta EC}$ mice compared with the Peli1$^{F/F}$ mice (Fig. 2c). Moreover, the lost number of microvessels induced by STZ was restored in Peli1$^{\Delta EC}$ mice compared with Peli1$^{F/F}$ mice (Fig. 2d). Endothelial dysfunction is often accompanied by cell apoptosis under diabetic conditions; however, endothelial specific deficiency of Peli1 protected endothelial cells from diabetes-induced apoptosis (Fig. 2e). Taken together, these data suggested that Peli1 deficiency in endothelium could attenuate diabetes-induced cardiac microvascular dysfunction.

3.3. Endothelial specific deficiency of Peli1 prevented cardiac remodeling

Since persistent hyperglycemia can induce ventricular dysfunction due to microvascular injury, we used fluorescence Oregon Green 488-labeled WGA staining to monitor the size of cardiomyocyte in diabetic mice at 16 week. Under diabetic conditions, cardiomyocyte developed hypertrophy (analyzed by cardiomyocyte cross-sectional area and HE staining) in Peli1$^{F/F}$ mice, but the hypertrophy of cardiomyocytes was

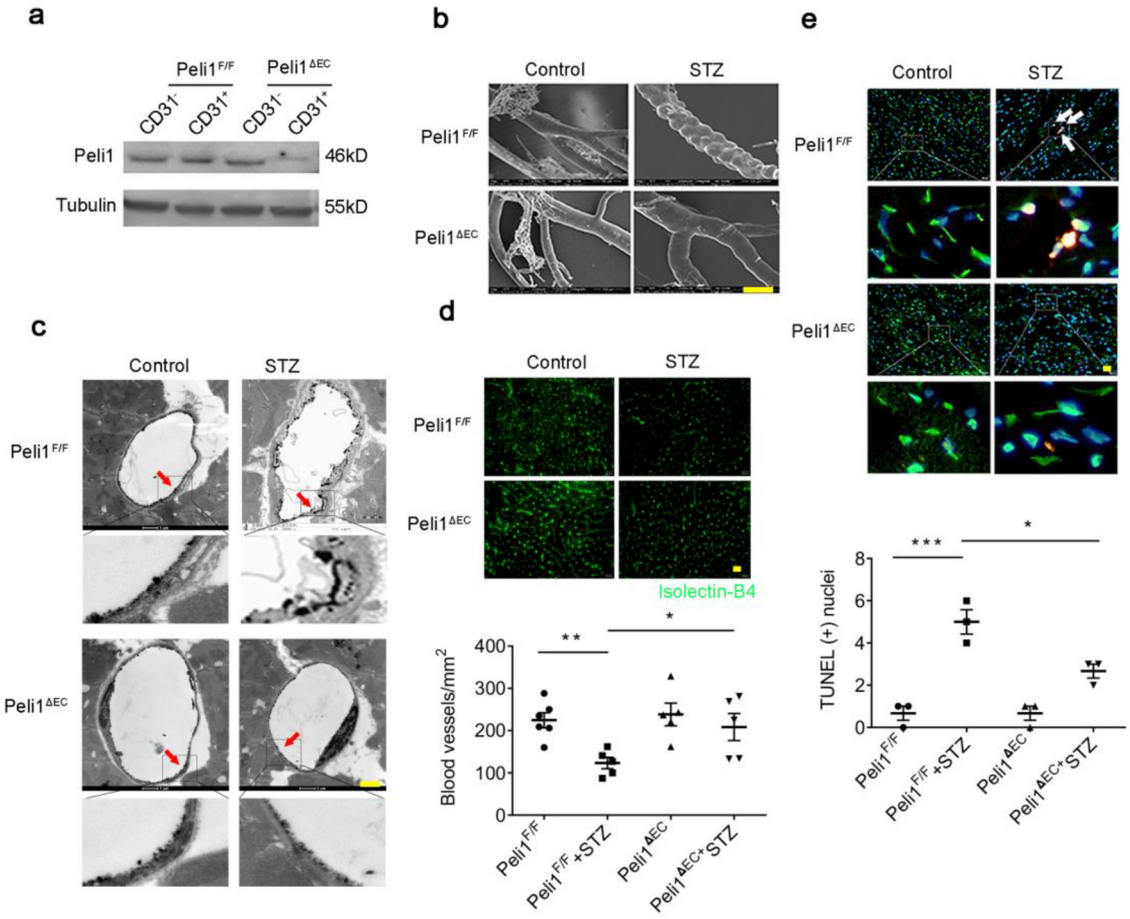

Fig. 2. Endothelial-specific deficiency of Peli1 attenuates cardiac microvascular injury.
Peli1$^{F/F}$ mice were crossed with Tie2-Cre mice to generate endothelial-specific deficiency Peli1 mice (Peli1$^{\Delta EC}$) and diabetes was induced by the injection of streptozotocin (STZ). (a). Endothelial cells (CD31^{+}) and other cells (CD31^{-}) were separated from the hearts of Peli1$^{F/F}$ and Peli1$^{\Delta EC}$ mice through MACS and Peli1 protein expression was determined by western blot. n = 3 (b). The surface and integrity of cardiac microvessels was observed by scanning electron microscope. Scale bar, 100 μm. n = 3 (c). The permeability of cardiac microvessels was detected by lanthanum nitrate and observed by transmission electron microscope (EM). Red arrows indicated the microvascular barrier dysfunction. Scale bar, 1 μm. n = 3 (d). Representative immunofluorescence staining of capillaries (green, Isolectin-B4). Scale bar, 20 μm; n = 5. (e). Representative photomicrographs of TUNEL (red) and nuclear (DAPI) staining of microvessels (green, Isolectin-B4). (Scale bar, 20 μm); n = 3. Data are expressed as mean ± SEM. $^{*}p < 0.05$, $^{**}p < 0.01$ and $^{***}p < 0.001$.

improved in Peli1$^{\Delta EC}$ mice compared with the Peli1$^{F/F}$ mice (Fig. 3a,b). Consistently, myocardial fibrosis around perivascular and interstitial regions, stained by Sirius Red, was also attenuated in Peli1$^{\Delta EC}$ mice (Fig. 3c). Next, we examined whether Peli1 deficiency in endothelium could preserve cardiac function. Diabetes significantly impaired systolic function in diabetic Peli1$^{F/F}$ mice compared with control, evidenced by decreased ejection fraction (EF%) (60.46 ± 0.85% vs. 51.92 ± 1.03%) and fractional shortening (FS%) (29.98 ± 0.59% vs. 23.22 ± 0.62%) after last STZ injection, respectively. However, these changes were reversed in diabetic Peli1$^{\Delta EC}$ mice (Fig. 3d). Concordantly, Pelil deficiency in endothelium improved cardiac diastolic function in diabetic mice, indicated by the increased E/A ratio (from 1.58 ± 0.04% to 1.76 ± 0.05%) (Fig. 3e). These results provided evidence that Pelil deficiency in endothelium could prevent cardiac remodeling under diabetic conditions, in which a regulation likely due to the protection of microvascular endothelium.

3.4. Peli1 knockdown in CMECs ameliorated AGEs-induced endothelial dysfunction

AGEs serve as a driving force of diabetic complications, including microvascular disorders. *Peli1* mRNA and protein levels were shown to increase with AGEs stimulation in cultured CMECs (Fig. 1g,h). To investigate the effect of Peli1 knockdown on cell-cell contacts, we examined the levels of several transmembrane junctional proteins, and found that Peli1 knockdown protected cell-cell contacts by reducing the loss of *Ve-cadherin* (encoded by Cdh5) expression and *Pecam-1* (encoded by CD31) expression in AGEs-treated CMECs (Fig. 4a,b). The permeability of CMECs was enforced by AGEs treatment with the increased flux of FITC-dextran and reduced TEER. However, Peli1 knockdown improved the permeability of AGEs-treated CMECs (Fig. 4c,d). To test the potential role of Peli1 in angiogenesis, Matrigel assay was performed. The results showed that Peli1 knockdown partially restored the ability of CMECs to form capillaries and promoted cell migration in the presence of AGEs (Fig. 4e,f). Finally, the effect of Peli1 on CMECs apoptosis in vitro was explored. Peli1 knockdown blocked caspase cascades by reducing the formation of cleaved caspase 12 and caspase 3 in CMECs (Fig. 4g,h). These results suggested that Peli1 knockdown may prevent CMECs from AGEs-induced endothelial dysfunction.

3.5. Peli1 knockdown suppressed IRE1α activation and downstream MAPK signaling in CMECs

IRE1α-mediated ER stress is associated with diabetic cardiac microvascular diseases. To verify whether Peli1 could affect microvascular injury via ER stress, we silenced Peli1 in CMECs by adv-shPeli1

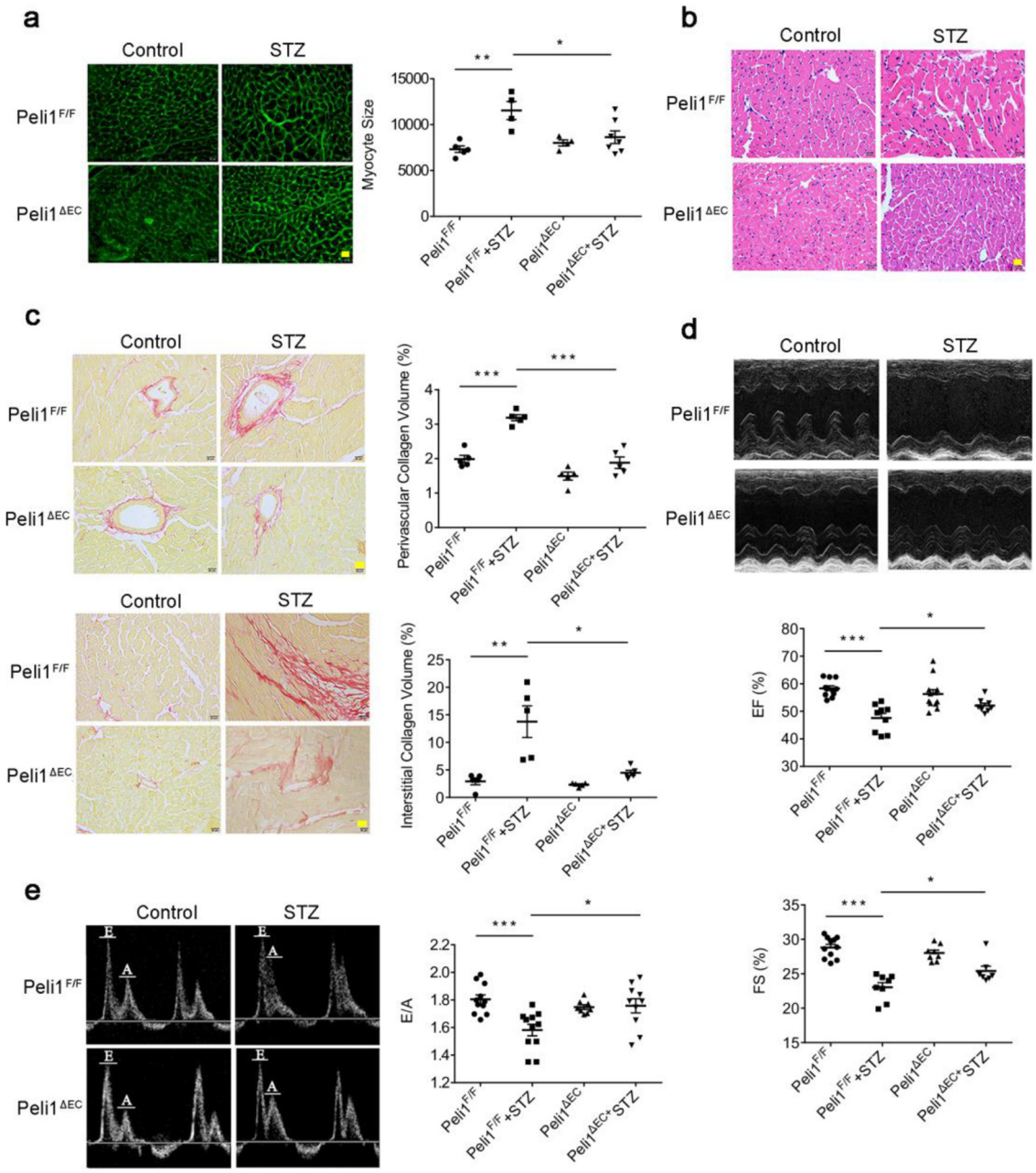

Fig. 3. Endothelial-specific deficiency of Peli1 attenuates cardiac remodeling.
Diabetes was induced by the injection of streptozotocin (STZ) inPeli1$^{F/F}$ and Peli1$^{\Delta EC}$ mice, and cardiac remodeling was detected at 16 week. (a) Representative WGA staining of cardiomyocytes. Scale bar, 20 μm; n = 4. (b) Representative HE staining of myocardial tissues. Scale bar, 20 μm. n = 3 (c). Sirius Red staining was applied to detect the deposition of collagen of perivascular and interstitial of heart section. Scale bar, 20 μm; n = 5. (d) Representative M-mode echocardiographic images; n = 10 (e) Representative echocardiographic images of mitral flow spectrum. n = 10. Data are expressed as mean ± SEM. $^{*}p < 0.05$, $^{**}p < 0.01$ and $^{***}p < 0.001$.

infection and with the treatment of AGEs. We found that IRE1α activation was reduced in CMECs with Peli1 knockdown, while p-PERK and ATF6, another two sensor proteins in UPR, were not affected (Fig. 5a). Consistently, Peli1 knockdown also attenuated the splicing and maturation of XBP1, a key step of ER stress response, and reduced the recruitment of TRAF2 to IRE1α (Fig. 5b,c). In response to IRE1α activation, MAPK activation mediates cell death in special tissues and cells. Peli1 knockdown in CMECs suppressed the activation of p38 and JNK (Fig. 5d). We isolated CMECs from Peli1$^{\Delta EC}$ and Peli1$^{F/F}$ mice, and found that IRE1α, p38 and JNK phosphorylation were enhanced in diabetic mice and were reduced in Peli1$^{\Delta EC}$ mice compared with Peli1$^{F/F}$ mice (Fig. 5e). Furthermore, immunofluorescence analyses confirmed that p-IRE1α in the vessels was dramatically increased in diabetic mice, but this increase was reversed in Peli1$^{\Delta EC}$ mice compared with Peli1$^{F/F}$ mice (Fig. 5f). In brief, these results indicated that Peli1 deficiency in endothelium could ameliorate endothelial dysfunction by blocking IRE1α phosphorylation.

3.6. Peli1 directly interacted with Hsp90

To explore the concrete mechanism that Peli1 promotes IRE1α activation, we expressed Flag-tagged Peli1 (Ad-Flag-Peli1) and control GFP (Ad-GFP) adenovirus in CMECs. Through immunoprecipitation with an anti-Flag antibody followed by PAGE electrophoresis, silver staining showed key differences between IgG and Flag-Peli1 (shown by red arrow). Mass spectrometry identified a peptide matching to hsp90

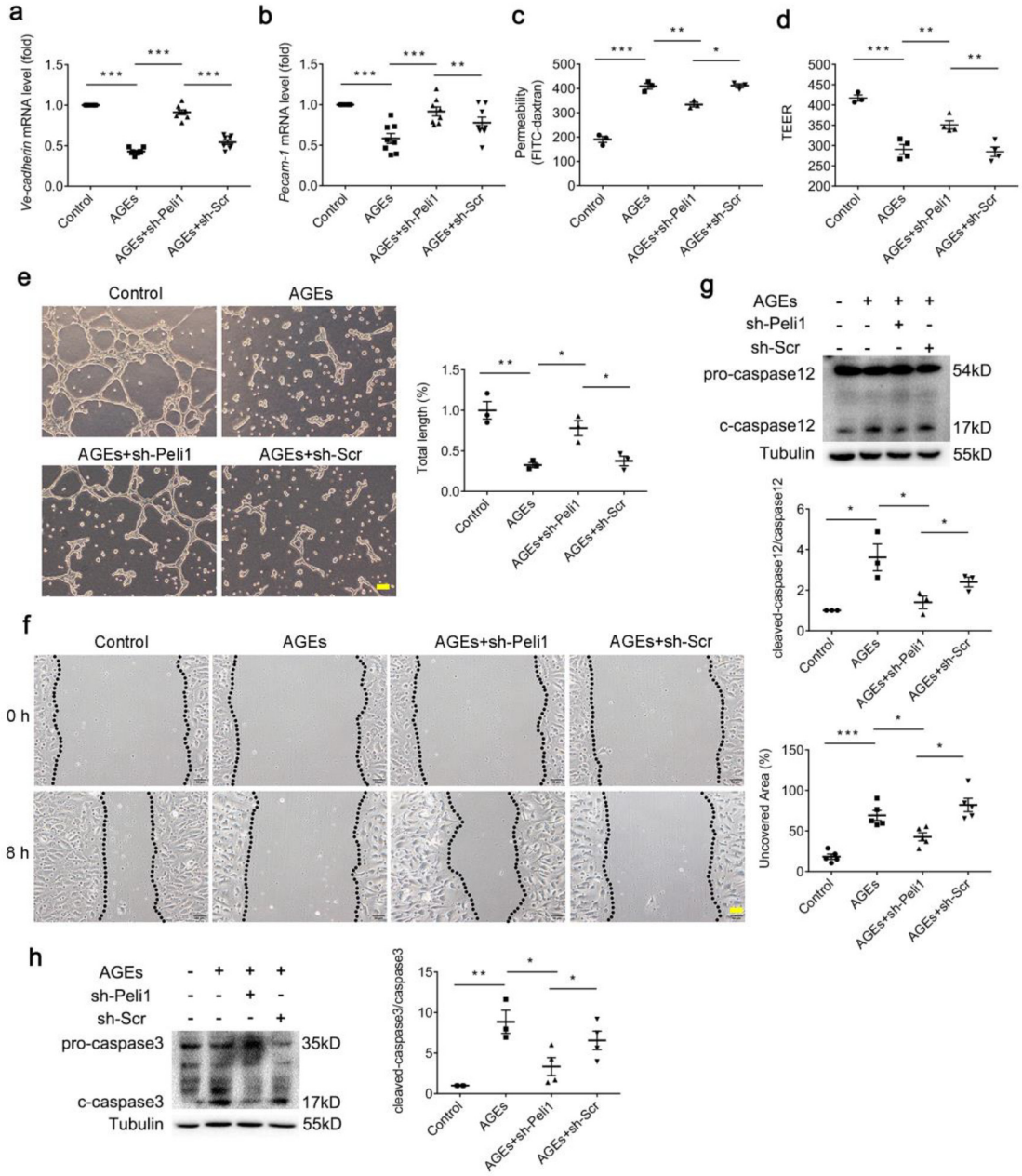

Fig. 4. Deletion of Peli1 in CMECs ameliorates AGEs-induced endothelial dysfunction.
CMECs were stimulated with advanced glycation end products (AGEs, 200 μg/ml) for 8 h after transfection with adv-shPeli1 or adv-shScr for 48 h. The mRNA levels of *Ve-cadherin* (a) and *Pecam1* (b) were detected by RT-qPCR analysis; n = 8. (c) The flux of four-kilodalton dextran flux in CMECs; n = 3. (d) Transendothelial electrical resistance (TEER) in CMECs; n = 4. (e) Capillary morphogenesis in CMECs with microscopy. Scale bar, 50 μm; n = 3. (f) Representative photomicrograph of CMECs migration through the cell scratch test. Scale bar, 50 μm; n = 5. The protein levels of cleaved-caspase12 (g) and cleaved-caspase3 (h) were detected by Western blot analysis; n = 3. Data are expressed as mean ± SEM. $^{*}p < 0.05$, $^{**}p < 0.01$ and $^{***}p < 0.001$.

in Peli1 immune complexes derived from cells, suggesting that Hsp90 might be a binding partner for Peli1 (Fig. 6a). Molecular dynamics simulation (MDS) was then conducted to explore the potential interaction sites between Peli1 and Hsp90. As shown in Fig. 6b, ARG-279, ARG-222, ARG-326, LYS-229 and LYS-374 might be the sites of Peli1 binding to Hsp90. To further validate explore the endogenous binding of Peli1 and Hsp90, we used co-immunoprecipitation assay with indicated antibodies in whole cell lysate in CMECs. In line with previous results, endogenous Peli1 and Hsp90 bound with each other in whole cell lysates of CMECs. Moreover, the binding of Peli1 and Hsp90 were increased with AGEs treatment. (Fig. 6c). Z-DOCK for protein structure modeling predicted that the Ring domain of Peli1 could interact with Hsp90. Next, we constructed Flag-tagged Full length Peli1 (aa 1-418, Flag-Peli1), Peli1 with deletion at FHA domain (aa 276-418, Flag-Peli1ΔFHA) and Peli1 with deletion at Ring domain (aa 1-289, Flag-Peli1ΔRing) (Fig. 6d). These adenoviruses were transfected in CMECs independently. Flag-Peli1 and Flag-Peli1ΔFHA showed clear interaction with Hsp90 by co-immunoprecipitation experiment, whereas Flag-Peli1ΔRing abolished their interaction with Hsp90 (Fig. 6e). GST pull-down assay was also conducted and the results showed strong binding of GST-Peli1 and GST-Peli1ΔFHA recombinant protein to HA-Hsp90, respectively (Fig. 6f).

3.7. Peli1 facilitates IRE1α phosphorylation via binding to Hsp90

Hsp90 binds to client proteins and regulates their stability and

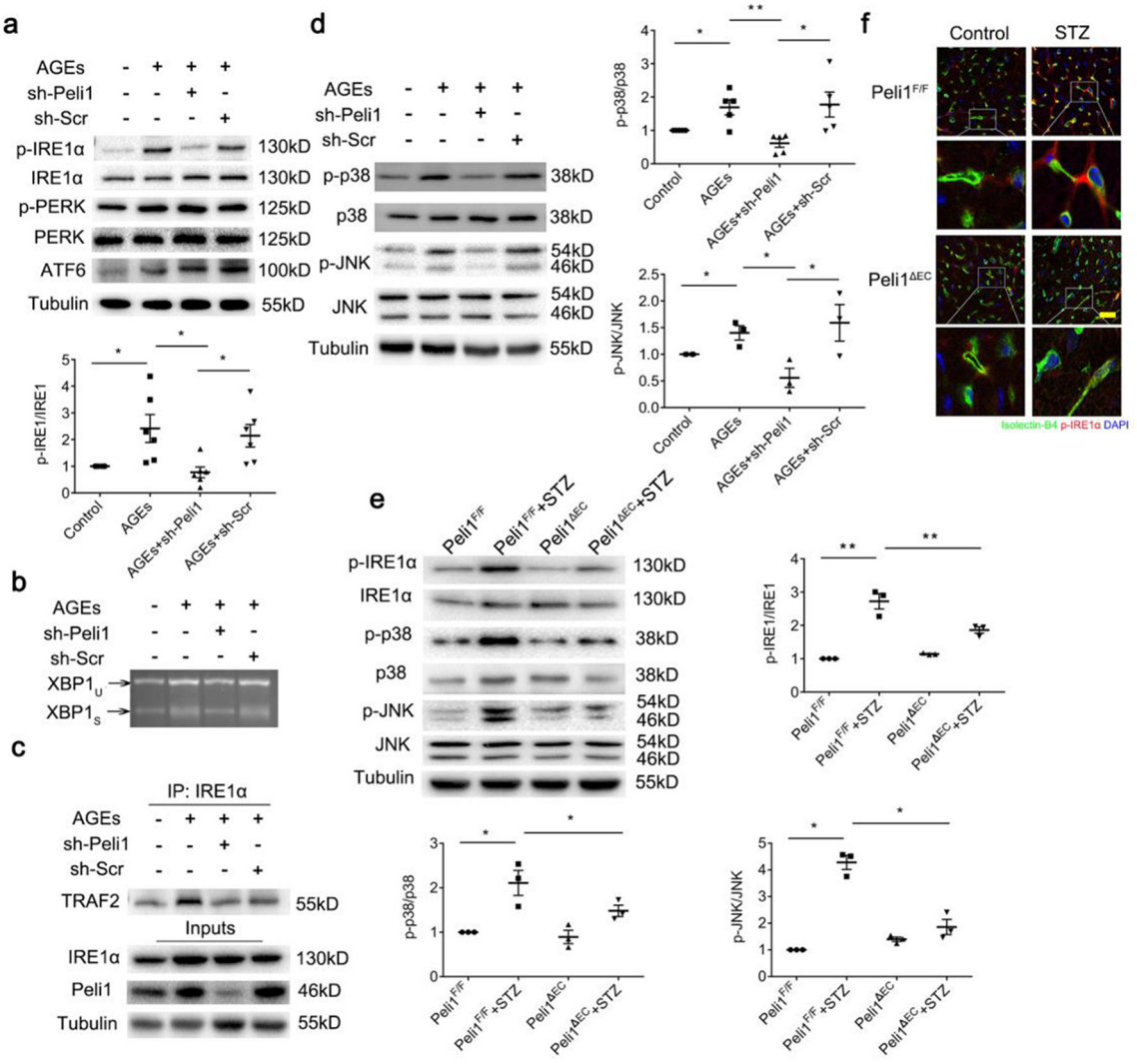

Fig. 5. Deletion of Peli1 decreases IRE1α phosphorylation in CMECs.
(a) Western blot analysis for ER stress signaling markers, including p-IRE1α, p-PERK and ATF6; n = 6. (b) Quantitative PCR of unspliced XBP1 ($XBP1_U$) and spliced XBP1 ($XBP1_S$); n = 3. (c) CMECs were infected with adv-shPeli1/adv-shScr and cell lysates were immunoprecipitated with an IRE1α antibody and analyzed by Western blot with TRAF2 antibody. n = 3. (d) The levels of phospho-p38 and phospho-JNK were determined by western blot analysis; n = 5. (e) The protein levels of phospho-IRE1α, phospho-p38 and phospho-JNK in endothelial cells separated from diabetic $Peli1^{F/F}$ and $Peli1^{\Delta EC}$ mice through Magnetic-activated cell sorting (MACS) were examined by Western blots using Tubulin as a loading control. n = 3. (f) The detection of p-IRE1α (red) on microvessels (green) was performed with immunofluorescence staining in diabetic $Peli1^{F/F}$ and $Peli1^{\Delta EC}$ mice. Scale bar, 20 μm. Data are expressed as mean ± SEM. $^{*}p < 0.05$ and $^{**}p < 0.01$.

functions. We then detected whether Peli1 activates IRE1α through directly binding to Hsp90. The stimulation of AGEs decreased the interaction between Hsp90 and IRE1α, whereas the alteration was reversed in CMECs with Peli1 deficiency (Fig. 7a). To further identify whether the association of Hsp90 and IRE1α depended on Peli1, we isolated CMECs from the $Peli1^{F/F}$ and $Peli1^{KO}$ mice respectively. As shown in Fig. 7b, the interaction between Hsp90 and IRE1α was dramatically increased in $Peli1^{KO}$ CMECs, compared with $Peli1^{F/F}$ CMECs. ZDOCK analysis also revealed that Peli1 and IRE1α shared the same binding sites on Hsp90 (purple domain), including VAL-17, THR-19, ILE-34, ASN-35, LYS-84, GLN-85, ASP-86, ARG-87, THR-88, GLU-146, LYS-147, GLU-163, ALA-166, GLY-167, SER-169, THR-171, ARG-173, HIS-189, LYS-191 and GLU-192, respectively (Fig. 7c,d). To get further insight into the function of Hsp90 in Peli1-induced IRE1α phosphorylation, we found that overexpression of Peli1 promoted the phosphorylation of IRE1α, whereas IRE1α phosphorylation was inhibited when Hsp90 and Peli1 were overexpressed simultaneously, regardless of the presence or absence of AGEs. Moreover, overexpression of Peli1 induced phosphorylation of p38 and JNK, but these effects were rescued when Hsp90 is overexpressed (Fig. 7e). To further confirm that endothelial cells-expressed Peli1 facilitates IRE1α phosphorylation via binding with Hsp90, we obstructed the function of Hsp90 in $Peli1^{KO}$ CMECs with Hsp90 inhibitor (17-AAG). As shown in Fig. 7f, the inhibition of Hsp90 largely reversed the limited IRE1α phosphorylation in $Peli1^{KO}$ CMECs. Therefore, we draw a conclusion that the effects of Peli1 on IRE1α phosphorylation are mediated at least in part by its direct binding to Hsp90 in CMECs ultimately leading to the dissociation of Hsp90 from IRE1α.

4. Discussion

Microvascular endothelial dysfunction is involved in altered cardiac structure and function under diabetic conditions [35]. Although multiple pathological factors, such as oxidative stress, inflammation and the impaired angiogenic capacity, simultaneously occur in the progression of this disease, the pathogenesis is unclear. We showed that Peli1 induction might be a common cause for these consequences. In response to persistent hyperglycemia, Peli1 induced ER stress by

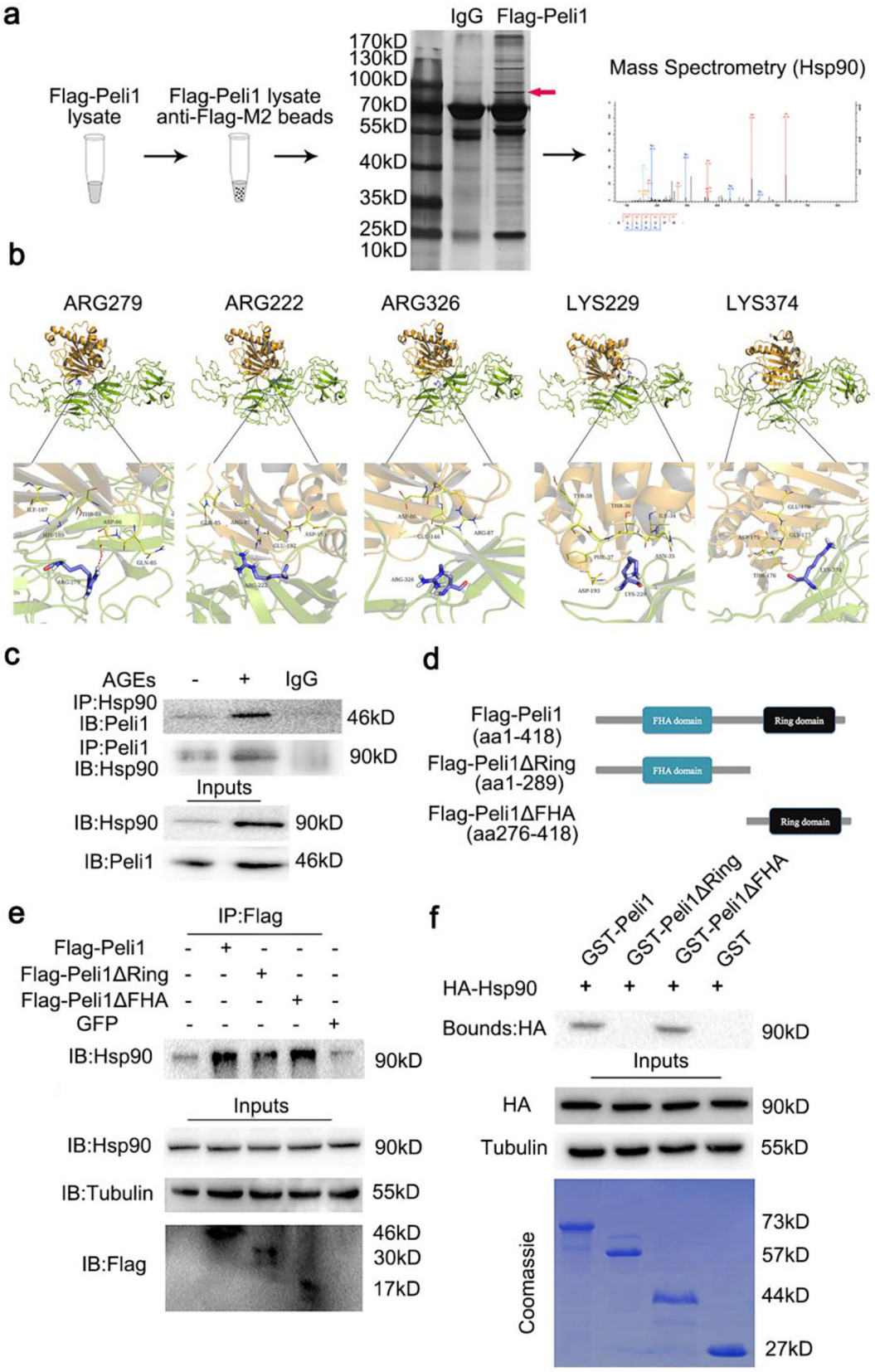

Fig. 6. Identification of Hsp90 as Peli1-binding partners. (a) Schematic representation of the pretreatment of samples for mass spectrometry. CMECs were infected with Ad-GFP or Ad-Flag-Peli1 for 48 h. Cell lysates were purified with anti-Flag affinity beads and eluted with Flag peptides. The eluates were resolved on SDS-PAGE and silver-stained. (b) Interaction pattern of these top five key amino acids (ARG-279, ARG-222, ARG-326, LYS-229, LYS-374) in Peli1 with Hsp90. (c) Co-IP analysis identified the combination of Hsp90 and Peli1 with or without AGEs stimulation (200 μg/ml); n = 6. (d) The diagram of Peli1 domain structure and mutants. (e) Ad-Flag-Peli1, Ad-Flag-Peli1ΔFHA and Ad-Flag-Peli1ΔRing were infected independently in cardiac microvascular endothelial cells (CMECs) for 48 h. Whole cell lysates from CMECs were immunoprecipitated with Flag, and then immunoblotted with antibodies against Hsp90; n = 6. (f) In vitro GST pull-down assay of GST, GST-Peli1 and GST-Peli1ΔFHA fusion proteins with HA-Hsp90 fusion protein. n = 3.

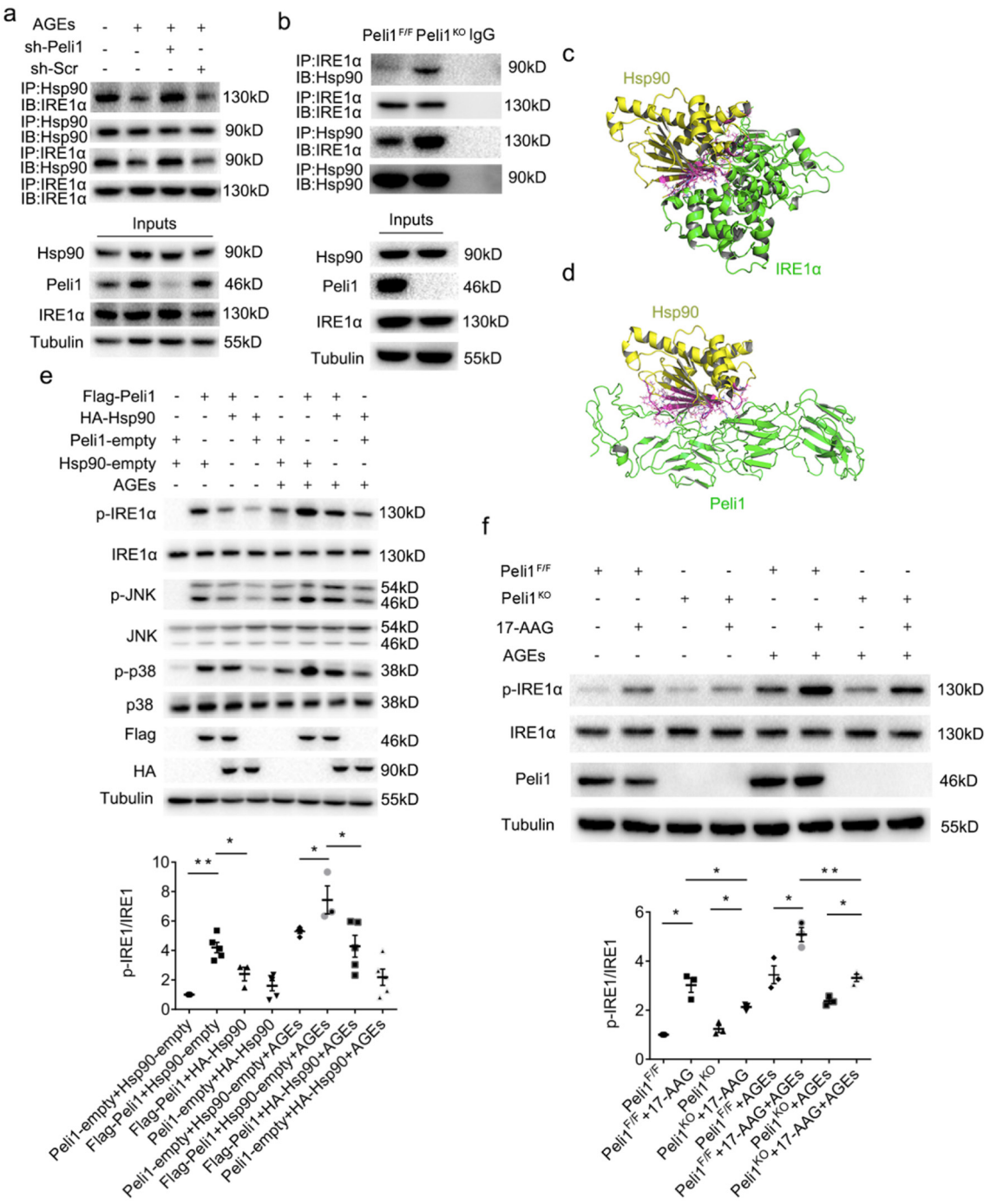

Fig. 7. Peli1 induced IRE1α phosphorylation by binding with Hsp90. (a) Ad-shPeli1 and Ad-Scr were infected in CMECs for 48 h before treated with AGEs (200 μg/mL) for another 8 h. Whole cell lysates from CMECs were immunoprecipitated with Hsp90 antibody or IRE1α antibody, and then immunoblotted with IRE1α and Hsp90 antibodies. n = 3. (b) The endothelial cells were separated from Peli1$^{F/F}$ mice or Peli1^{KO} mice. Co-IP assay between endogenous Hsp90 and endogenous IRE1α. n = 3 (c) The specific binding sites of Hsp90 (yellow) with IRE1α (green) through protein docking. (d) The specific binding sites of Hsp90 (yellow) with Peli1 (green) through protein docking. (e) Plasmid of HA-Hsp90 or HA-empty was co-transfected with Flag-Peli1 or Flag-empty plasmid with AGEs stimulation in HEK293A cells for 36 h as indicated. Whole-cell lysates were immunoblotted with antibodies against p-IRE1α, IRE1α, p-JNK, JNK, p-p38, p38, Flag and HA respectively. n = 5 (f) The endothelial cells were separated from Peli1$^{F/F}$ or Peli1^{KO} mice respectively with or without 17-AAG (1 μmol/L) treatment in the absence or presence of AGEs. Whole cell lysates were immunoblotted with antibodies against p-IRE1α, IRE1α, Peli1 and Tubulin; n = 3. Data are expressed as mean ± SEM. $^{*}p < 0.05$ and $^{**}p < 0.01$.

activating IRE1α signaling branch in a Hsp90-dependent manner, and impaired cardiac structure and function due to the damage of cardiac microvessels.

Peli1 is a member of the pelle-interacting protein family and regulates innate immune signaling. Peli1 serves as a vital mediator of Toll-like receptors [25]. In diabetic mice, we found that Peli1 induction was correlated with cardiac microvascular injury, suggesting the contributions to endothelial dysfunction and cardiac injury. Because protein glycation is formed due to persistent hyperglycemia under diabetic conditions, Peli1 induction in CMECs by AGEs stimulation established the association of Peli1 induction with microvascular dysfunction in diabetes. Although previous studies have found that Peli1 induction is

instigated by inflammatory signaling [36–38], it remains undetermined how Peli1 works in the microvascular endothelial cells in response to a hyperglycemic microenvironment. Endothelial dysfunction in diabetes mellitus is characterized by the impaired microvascular connection and integrity [39]. In contrast to our findings of the cardiac microvessels and endothelial cells, it has been previously reported that adenovirus-mediated Peli1 overexpression in ischemic heart to impaired collateral blood vessels formation, possibly resulting from non-specific up-regulation of Peli1 [40]. However, in our study, Peli1 depletion was specific in the endothelial cells of cardiac microvessels and resulted in endothelial dysfunction and cardiac remodeling in the context of hyperglycemia. These discrepancies in aggregate appear to argue for a cell-specific, context-dependent role for Peli1 in the regulation of cardiovascular pathophysiology. Additional studies are necessary to dissect the cell-autonomous and non-cell-autonomous roles of Peli1 in the cardiovascular system.

Different mechanisms may account for cardiac microvascular dysfunction under diabetic conditions and ER stress emerges as a potential cause for these events. IRE1α, PERK and ATF6 are transmembrane proteins, sensing the accumulation of unfolded proteins to induce ER stress through different signaling pathways [41]. Although AGEs stimulation increased phosphorylation of IRE1α and PERK and induction of ATF6 in CMECs, Peli1 deficiency in CMECs only diminished AGEs-induced IRE1α phosphorylation, indicating that Peli1 mediated AGEs-induced ER stress in a specific way through IRE1α signaling branch. The IRE1α-TRAF2 complex can recruit p38 and JNK to induce inflammation and apoptosis [42,43]. In this study, Peli1 deficiency in CMECs did protect endothelial cells from AGEs-induced cell apoptosis, permeability and regeneration by suppressing JNK and p38 activation. The signal pathways and molecular mechanisms of apoptotic regulation are extremely complex. Previous study also found that Peli1 may promote apoptosis through modulating noncanonical NF-κB or modulating RIP1 or RIP3 ubiquitination [44–46]. The mechanisms may include, but not limited to these signaling molecules, so this needs further study in the future. Taken together, these results provide evidence that Peli1 promotes cardiac microvascular dysfunction through IRE1α/MAPK pathway under diabetic conditions.

Hsp90 is a highly abundant and ubiquitous molecular chaperone mediating cellular responses. Hsp90 is required for the correct maturation and activation of a number of key cellular proteins and protein complexes, which are collectively called “clients”. Many of the Hsp90 clients are either kinases or transcription factors involved in the regulation of ER stress [47]. In fact, the molecular chaperone Hsp90 regulates stability and function of multiple protein kinases. It is demonstrated that Hsp90 combines with and stabilizes IRE1α, and thus prevents ER stress via limiting IRE1α phosphorylation [48]. In the present study, we identified Hsp90 as a Peli1 binding protein by LC/MS-MS. In addition, we found that Peli1 interacts with Hsp90 via the Ring domain. Molecular dynamics simulation analysis revealed five amino acids (ARG279, ARG222, ARG326, LYS229 and LYS374) within the Ring domain of Peli1 contributing to the combination of free binding energy during the Hsp90-Peli1 interaction. Our study also indicated that Peli1 deficiency in CMECs prevents Hsp90 dissociating from IRE1α to reduce IRE1α phosphorylation.Hsp90 is located in the endoplasmic reticulum, and therefore, we speculated that the Ring domain of Peli1 binds to Hsp90 to free IRE1α for activation, mediating ER stress-associated endothelial dysfunction under diabetic conditions.

In summary, our results reveal an unrecognized role of Peli1 in diabetes-induced cardiac microvascular injury and demonstrate that Peli1 in endothelium could aggravate cardiac microvascular dysfunction by directly binding to Hsp90 to activate IRE1α. These findings raise the possibility that Peli1 could be a novel target in the treatment of diabetes-induced cardiac microvascular dysfunction.

Funding

This work was supported by the National Natural Science Foundation of China (81770230; 81470418; 81725001).

Contribution statement

Yuehua Li and Yong Xu designed the experiments and interpreted the results. Qianwen Zhao performed experiments and wrote the manuscript. Jie Yang, Hao Chen, Jiantao Li, Xiaolu Wang and Linli Que performed experiments and analyzed data. Guoqing Zhu, Tuanzhu Ha and Li Liu contributed to the discussion and critical revision of the manuscript. Qi Chen and Chuanfu Li helped to search literature and reviewed the manuscript. All authors approved the final version of the paper.

Transparency document

The Transparency document associated with this article can be found, in online version.

Data availability

The data that support the findings of this study are available from the corresponding author upon reasonable request.

Declaration of Competing Interest

The authors declare that there are no conflicts of interest with this manuscript.

Acknowledgments

We thank Dr. Jinfeng Liu from China Pharmaceutical University for helping with protein docking and molecular dynamics simulation. We also thank Dr. Baolin Liu from China Pharmaceutical University for helping revising this paper.

Appendix A. Supplementary data

Supplementary data to this article can be found online at https://doi.org/10.1016/j.bbadis.2019.06.017.

References

[1] Huang ES, Basu A, O'Grady M, Capretta JC(2009)Projecting the future diabetes population size and related costs for the U.S. Diabetes Care32:2225–2229.
[2] Rawshani A, Sattar N, Franzen S et al (2018) Excess mortality and cardiovascular disease in young adults with type 1 diabetes in relation to age at onset: a nation-wide, register-based cohort study. Lancet392:477–486.
[3] Scarabelli T, Stephanou A, Rayment N et al(2001) Apoptosis of endothelial cells precedes myocyte cell apoptosis in ischemia/reperfusion injury. Circulation104:253–256.
[4] Marfella R, Esposito K, Nappo F et al (2004) Expression of angiogenic factors during acute coronary syndromes in human type 2 diabetes. Diabetes53:2383–2391.
[5] Adameova A, Dhalla NS (2014) Role of microangiopathy in diabetic cardiomyopathy. Heart Fail Rev19:25–33.
[6] Ceradini DJ, Yao D, Grogan RH et al (2008) Decreasing intracellular superoxide corrects defective ischemia-induced new vessel formation in diabetic mice.J BiolChem283:10930–10938.
[7] Wang D, Luo P, Wang Y et al (2013) Glucagon-like peptide-1 protects against cardiac microvascular injury in diabetes via a cAMP/PKA/Rho-dependent mechanism. Diabetes62:1697–1708.
[8] Quan A, Pan Y, Singh KK et al (2017) Cardiovascular inflammation is reduced with methotrexate in diabetes. Mol Cell Biochem432:159–167.
[9] Wang M, Kaufman RJ (2014) The impact of the endoplasmic reticulum protein-folding environment on cancer development. Nat Rev Cancer14:581–597.
[10] Doroudgar S, Glembotski CC (2013) New concepts of endoplasmic reticulum function in the heart: programmed to conserve. J Mol Cell Cardiol55:85–91.
[11] Elmasry K, Ibrahim AS, Saleh H et al (2018) Role of endoplasmic reticulum stress in 12/15-lipoxygenase-induced retinal microvascular dysfunction in a mouse model of diabetic retinopathy. Diabetologia61:1220–1232.

[12] H. Zhou, J. Wang, P. Zhu, S. Hu, J. Ren, Ripk3 regulates cardiac microvascular reperfusion injury: the role of IP3R-dependent calcium overload, XO-mediated oxidative stress and F-action/filopodia-based cellular migration, Cell. Signal. 45 (2018) 12–22.
[13] R. Sano, J.C. Reed, ER stress-induced cell death mechanisms, BiochimBiophysActa 1833 (2013) 3460–3470.
[14] Shi L, Wang Z, Liu X, Li M, Zhang S, Song X (2018) Bax inhibitor-1 is required for resisting the Early Brain Injury induced by subarachnoid hemorrhage through regulating IRE1-JNK pathway. Neurol Res40:189–196.
[15] Liu L, Qi X, Chen Z et al(2013) Targeting the IRE1α/XBP1 and ATF6 arms of the unfolded protein response enhances VEGF blockade to prevent retinal and choroidal neovascularization. Am J Pathol182:1412–1424.
[16] M.G. Marcu, M. Doyle, A. Bertolotti, D. Ron, L. Hendershot, L. Neckers, Heat shock protein 90 modulates the unfolded protein response by stabilizing IRE1alpha, Mol Cell Biol22 (2002) 8506–8513.
[17] Singh R, Barden A, Mori T, Beilin L (2001) Advanced glycation end-products: a review. Diabetologia44:129–146.
[18] Ohtsu A, Shibutani Y, Seno K, IwataH, Kuwayama T, Shirasuna K (2017) Advanced glycation end products and lipopolysaccharides stimulate interleukin-6 secretion via the RAGE/TLR4-NF-κB-ROS pathways and resveratrol attenuates these inflammatory responses in mouse macrophages. ExpTher Med14:4363–4370.
[19] Witko-Sarsat V, Friedlander M, Nguyen Khoa T et al (1998) Advanced oxidation protein products as novel mediators of inflammation and monocyte activation in chronic renal failure. J Immunol161:2524–2532.
[20] L.M.O. Caram, R. Ferrari, D.L. Nogueira, et al., Tumor necrosis factor receptor 2 as a possible marker of COPD in smokers and ex-smokers, Int J Chron Obstruct Pulmon Dis12 (2017) 2015–2021.
[21] C. Wang, S.M. Armstrong, M.G. Sugiyama, et al., Influenza-induced priming and leak of human lung microvascular endothelium upon exposure to Staphylococcus aureus, Am J Respir Cell MolBiol 253 (2015) 459–470.
[22] Yang Q, Kim YS, Lin Y, Lewis J, Neckers L, Liu ZG (2006) Tumour necrosis factor receptor 1 mediates endoplasmic reticulum stress-induced activation of the MAP kinase JNK. EMBO Rep7:622–627.
[23] Hetz C (2012) The unfolded protein response: controlling cell fate decisions under ER stress and beyond. Nat Rev Mol Cell Biol13:89–102.
[24] Schauvliege R, Janssens S, Beyaert R (2007) Pellino proteins: novel players in TLR and IL-1R signalling.J Cell Mol Med11:453–461.
[25] P.N. Moynagh, The Pellino family: IRAK E3 ligase with emerging roles in innate immune signaling, Trends Immunol. 30 (2009) 33–42.
[26] Y. Xiao, J. Jin, M. Chang, et al., Peli1 promotes microglia-mediated CNS inflammation by regulating Traf3 degradation, Nat. Med. 19 (2013) 595–602.
[27] Qiu Q, Zheng Z, Chang L et al (2013) Toll-like receptor-mediated IRE1α activation as a therapeutic target for inflammatory arthritis. EMBO J32:2477–2490.
[28] Wu W, Hu y, Li J et al (2014) Silencing of Peli1 improves post-infarct cardiac dysfunction and attenuates left ventricular remodelling in mice. Cardiovasc Res102:46–55.
[29] Alabi RO, Glomski K,Haxaire C,Weskamp G, Monette S, Blobel CP (2016) ADAM10-dependent signaling through Notch1 and Notch4 controls development of organ-specific vascular beds. Circ Res119:519–531.
[30] Ryzhov S,Solenkova NV,Goldstein AE et al (2008) Adenosine receptor-mediated adhesion of endothelial progenitors to cardiac microvascular endothelial cells. Circ Res102:356–363.
[31] CaoZ, Hu Y, Wu W et al (2009) The TIR/BB-loop mimetic AS-1 protects the myocardium from ischaemia/reperfusion injury. Cardiovasc Res84:442–451.
[32] Hudson N, Powner MB, Sarker MH et al (2014) Differential apicobasal VEGF signaling at vascular blood-neural barriers. Dev Cell30:541–552.
[33] Wei L, Sun D, Yin Z et al (2010) A PKC-beta inhibitor protects against cardiac microvascular ischemia reperfusion injury in diabetic rats.Apoptosis15:488–498.
[34] Caporali A,Meloni M,Nailor Aet al (2015) p75(NTR)-dependent activation of NF-κB regulates microRNA-503 transcription and pericyte-endothelial crosstalk in diabetes after limb ischaemia. Nat Commun6:8024.
[35] Maamoun H, Zachariah M, McVey JH, Green FR, Agouni A (2017) Heme oxygenase (HO)-1 induction prevents endoplasmic reticulum stress-mediated endothelial cell death and impaired angiogenic capacity. BiochemPharmacol127:46–59.
[36] X. Ye, D. Kong, J. Wang, et al., MyD88 contributes to neuroinflammatory responses induced by cerebral ischemia/reperfusion in mice, BiochemBiophys Res Commun480 (2016) 69–74.
[37] Murphy M, Xiong Y, Pattabiraman G, Qiu F, Medvedev AE (2015) Pellino-1 positively regulates toll-like receptor (TLR) 2 and TLR4 signaling and is suppressed upon induction of endotoxin tolerance. J BiolChem290:19218–19232.
[38] Rednam CK, Wilson RL, Selvaraju V et al (2017) Increased survivability of ischemic skin flap tissue in Flk-$1^{+/-}$ mice by Pellino-1 intervention. Microcirculation24:e12362.
[39] De Galan BE, Hoekstra JB (2001) Glucose counterregulation in type 2 diabetes mellitus. Diabet.Med18:519–527.
[40] Thirunavukkarasu M,Selvaraju V,Joshi M et al (2018) Disruption of VEGF mediated Flk-1 signaling leads to a gradual loss of vessel health and cardiac function during myocardial infarction: potential therapy with Pellino-1. J Am Heart Assoc7:e007601.
[41] Xu J, Wang G, Wang Y et al (2009) Diabetes- and angiotensin II-induced cardiac endoplasmic reticulum stress and cell death: metallothionein protection. J Cell Mol Med13:1499–1512.
[42] Hu P, Han Z, Couvillon AD, Kaufman RJ, Exton JH (2006) Autocrine tumor necrosis factor alpha links endoplasmic reticulum stress to the membrane death receptor pathway through IRE1alpha-mediated NF-kappaB activation and down-regulation of TRAF2 expression. Mol Cell Biol26:3071–3084.
[43] Davis RJ (2000) Signal transduction by the JNK group of MAP kinases. Cell103:239–252.
[44] J. Liu, X. Huang, S. Hao, et al., Peli1 negatively regulates noncanonical NF-κB signaling to restrain systemic lupus erythematosus, Nat. Commun. 9 (2018) 1136.
[45] H. Wang, H. Meng, X. Li, et al., PELI1 functions as a dual modulator of necroptosis and apoptosis by regulating ubiquitination of RIPK1 and mRNA levels of c-FLIP, Proc Natl AcadSci U S A. 114 (2017) 11944–11949.
[46] S.W. Choi, H.H. Park, S. Kim, et al., PELI1 selectively targets kinase-active RIP3 for ubiquitylation-dependent proteasomal degradation, Mol. Cell 70 (2018) 920–935.
[47] Manni S, Brancalion A, Tubi LQet al (2012) Protein kinase CK2 protects multiple myeloma cells from ER stress-induced apoptosis and from the cytotoxic effect of HSP90 inhibition through regulation of the unfolded protein response. Clin Cancer Res18:1888–1900.
[48] Ota A, Wang Y (2012) Cdc37/Hsp90 protein-mediated regulation of IRE1 protein activity in endoplasmic reticulum stress response and insulin synthesis in INS-1 cells. J BiolChem287:6266–6274.